Escola d'Enginyeria de Telecomunicació i Aeroespacial de Castelldefels
UNIVERSITAT POLITÈCNICA DE CATALUNYA

TREBALL FINAL DE GRAU

TÍTOL DEL TFG: Experimental study of the main component of a technology for its use in space propulsion at cryogenic conditions

TITULACIÓ: Grau en Enginyeria d'Aeronavegació

AUTOR: Guillermo Gallego Chacón

DIRECTOR: Jose E. Garcia & Ricard González Cinca

DATA: 28 de juny del 2017

Título: Estudio experimental del principal componente de una tecnología para su uso en propulsión espacial en condiciones criogénicas.

Autor: Guillermo Gallego Chacón

Director: Jose E. Garcia & Ricard González Cinca

Fecha: 28 de junio del 2017

Resumen

A medida que la tecnología aeroespacial avanza, van surgiendo nuevos retos que hay que gestionar y solucionar para poder llevar a cabo futuras misiones de exploración espacial. Este estudio se enfrenta a uno de estos retos: el almacenamiento eficiente de combustible criogénico durante largo tiempo. Actualmente no hay tecnología suficiente para garantizar el aislamiento térmico en todo el transcurso de una misión, meses en ocasiones. Por ejemplo, se da por hecho la perdida de combustible por ebullición. Sin embargo existe una necesidad imperiosa de controlar las burbujas generadas por la ebullición, por dos motivos: la pérdida de miles de litros de combustible y pueden generar espumas peligrosas en diferentes momentos de la misión. Una de las tecnologías propuestas por el laboratorio de Microgravedad de la UPC para controlar y eliminar burbujas es el uso de ondas acústicas ultrasónicas, creadas por dispositivos piezoeléctricos. El componente principal de un dispositivo de ultrasonidos es el material piezoeléctrico activo. Por ello, el objetivo de este estudio consiste en encontrar un material piezoeléctrico que funcione correctamente a temperaturas criogénicas para obtener el control de burbujas en un líquido. Nuestra hipótesis inicial se basa en la posibilidad de controlar la formación de burbujas y la dinámica de ebullición en los tanques de combustible criogénico a partir de ondas acústicas generadas por un dispositivo piezoeléctrico

Hoy en día no se conocen cerámicas piezoeléctricas que trabajen de forma eficiente y duradera a temperaturas tan bajas. De hecho, el efecto piezoeléctrico apenas ha sido estudiado a estas temperaturas, probablemente por falta de aplicaciones. Sin embargo, sí que hay estudios sobre el control de burbujas en un líquido a partir de ondas acústicas en micro gravedad. La búsqueda de un material piezoeléctrico válido para esta finalidad supone un reto sin ninguna garantía de éxito. No obstante, en caso de encontrarse, esté podría ser utilizado en misiones espaciales.

Este estudio forma parte de un proyecto de investigación subvencionado por el gobierno por su originalidad e innovación dentro del sector aeroespacial, dado que es el primero en enfocar este problema a las

condiciones reales de temperaturas criogénicas. Y es el primero en enfocarse principalmente en las condiciones criogénicas. Para poder llevar a cabo el estudio se ha adquirido una serie de cerámicas piezoeléctricas, escogidas específicamente por sus propiedades, para realizar los experimentos.

Los resultados se han obtenido en el laboratorio de Materiales Piezoeléctricos del Departamento de Física de la UPC. Los resultados obtenidos no han sido muy prometedores, ya que las propiedades de todas las cerámicas piezoeléctricas estudiadas, decrecen fuertemente al decrecer la temperatura hasta llegar a unos mínimos que no permiten el funcionamiento deseado a las temperaturas necesarias. Por tanto, la utilización de estas cerámicas, que por su diseño eran muy prometedoras, se descarta por insuficiente respuesta piezoeléctrica. Sin embargo, no se descarta el objetivo del proyecto, ya que hay otros posibles materiales, como cristales piezoeléctricos que podrían llegar a funcionar a estas temperaturas.

Title: Experimental study of the main components of a technology for its use in space propulsion at cryogenic conditions

Author: Guillermo Gallego Chacón

Director: Jose E. Garcia & Ricard González Cinca

Date: 28 of June of 2017

Overview

As the aerospace technology progresses, new challenges emerge which have to be managed and solved to make future space exploration missions possible. This study faces one of these challenges: The efficient long-term storage of cryogenic propellant. Nowadays the available technology is not sufficiently evolved to ensure thermal isolation throughout the entire mission which can be months or even years. It's a given fact that propellant lost due to boil-off will happen. This inevitably calls for the imperative necessity of controlling the bubbles generated by the boiling for two reasons: Firstly, to avoid the loss of thousands of litres of propellant and secondly to prevent the possible generation of foam structures, which could be hazardous at different stages of the mission. Ones of the technology proposed by the UPC Microgravity laboratory to control and eliminate the bubbles is based on the use of ultrasonic acoustic waves, created by piezoelectric devices. The objective of this study is to find a piezoelectric material that works correctly at cryogenic temperatures, more exactly at -253ºC which is the boiling temperature of liquid hydrogen, to obtain the control of the bubbles in the liquid. Our initial hypothesis is based on the possibility of controlling the bubble formation and dynamics in boiling in cryogenic propellant storage tanks by means of an acoustic wave generated by a piezoelectric device.

At present, there isn't any piezoelectric ceramic material that works efficiently and is durable at such low temperatures. In fact, the piezoelectric effect has barely been studied at these temperatures, probably due to the lack of applications. However, there are studies about bubble control in liquids by means of acoustic waves in microgravity. The research for a good piezoelectric material for this purpose turns out to be a challenge without any guaranteed success. On the other hand, if such a material was found, it could be used in future space missions.

This study is part of an investigation project subsidized by the government for its originality and innovation in the aerospace sector, due to it's the first to focus this problem to the real conditions at cryogenic conditions. Its main focus is on the cryogenic conditions of fluids. To carry out the study, piezoelectric ceramics have been procured and selected specifically for their promising properties, to carry out the intended experiments.

The measurements were obtained in the Piezoelectric Materials laboratory of Physics Department of the UPC. The results show that the intended application is not feasible, since the piezoelectric properties of all ceramic materials studied have been decreasing exponentially with temperature up to a minimum at which the desired performance in the targeted range of operating temperatures doesn't appear at all.

We conclude that the use of these ceramics, which by its design were initially very promising, must be discarded for the insufficient piezoelectric response under cryogenic conditions. However, the aim of the project is not completely discarded, since there are other possible materials, like piezoelectric crystals that could work as required at very low temperatures.

Index

Figure & Table index

Acronyms Table

BCTZ: Barium Calcium Titanate Zirconate

PZT: Lead Zirconate Titanate

LCR: Inductance, Capacitance and Resistance

AC: Alternating Current

UPC: Universitat Politècnica de Catalunya

1. Introduction

The humans' desire to travel to other planets or undertake long trips through space, originates the imperative necessity to develop new technologies capable of carrying out this important aim. In long distance missions, for example to Mars, problems arose associated with the long-term storage of propellant such as the losses due to boil-off. The vapour bubbles generated inside the fuel tank can create dangerous problems at different phases of the operations. Nowadays not enough technology does exist to ensure the thermal isolation of all cryogenic propellant tanks for a long time. A technique has to be developed in order to control these vapour bubbles. One, which could allow us to control and eliminate the bubbles, is by making use of acoustic fields, currently under development at the UPC Microgravity Laboratory. A piezoelectric device generates an acoustic wave capable of retaining and moving the vapour bubbles to another part of the tank where the liquid is subcooled and where they collapse. In order to implement this technique in space, first it has to be tested under cryogenic conditions. However, there isn't any material which has been proven to have piezoelectric properties at 20 K, which is the Hydrogen boiling temperature.

It's crucial to find a solution to control the vapour bubbles, since the feasibility of using liquid propellant engines based on liquid hydrogen (LH2) and long range missions depend on it. Nowadays it's possible to reduce the boil off rate to below 3% per month. Despite this, the issue becomes a challenge when the mission has duration of 6 months or more. Current heat insulation techniques are not sufficient and further bubble control techniques are required.

The purpose of this study is to find some material that would show a sufficient piezoelectric behaviour at cryogenic temperatures, to sustain minimum losses of fuel for several months.

To carry out the study we have chosen different materials to test their piezoelectric properties at cryogenic temperature. These materials are commercial and non-commercial, the latter specially created to theoretically have good piezoelectric properties at low temperatures. Also, the non-commercial are lead-free ceramic materials to avoid the contamination that lead generates. The process of obtaining measurements has been done in the Piezoelectric Materials laboratory of Physics Department of the UPC, which is equipped with two vacuum pumps, a compressor and a cryogenic station. But, to obtain correct measurements, the samples have to undergo previously a preparation process.

This study consists of a brief historical review of piezoelectricity and ultrasounds, followed by an explanation of the materials that have been chosen for this work and the reasons of their selection. And finally, the discussion of the measurements and the results.

1.1. Historical Context

Ultrasound development truly began with the creation of subaquatic transducers, for the detection of submarines in World War I. Their actual discovery happened in the XVIll century. The psychologist and priest Lazzaarro Spallanzani (1729-1799), was the first one to realize that we are surrounded by sounds inaudible for the human ears [1]. But it was in 1794 when he bore out his ideas thanks to an experiment done with bats, where he noticed that instead of vision, these animals used their hearing to locate and catch objects in the air and to be able to fly without crashing. Later it was discovered that bats emit sound waves that collide with objects whose echoes return to be captured by their ears and processed by their brains. This type of orientation is called echo-localization.

In 1881, Pierre Curie with his brother Jacques Curie discovered that some crystals reacted generating an electric potential when mechanical stress was applied on them. This behaviour is known as piezoelectric effect. Afterwards, Curie brothers demonstrated the inverse effect; that crystals could deform when electric stress was applied [2]. They also observed that this effect was usually reversible and when crystals were no longer subject to an electric field and that they returned to their original form. This scientific achievement was the beginning for the creation of what is nowadays known as ultrasound transducers.

From its discovery until today the studies about the piezoelectric phenomenon have had periods of quick progress. Paul Langevin, a French physicist, invented the first echo-localizer to detect icebergs, just after the Titanic sank in 1912. This invention was called Hydrophone and was the first ultrasound transducer. The Langevin transducer consisted in a quartz layer placed between two steel sheets which could generate ultrasound waves. It was a device capable of sending and receiving high frequency waves. Later the Hydrophone was used in World War I, for the detection of foe submarines (SONAR: Sound Navigation And Ranging). In this period, new piezoelectric materials such as Barium Titanate (BT) and Lead Zirconate Titanate (PZT) were discovered, which allowed a significant step forward in the use and application of piezoelectric materials in different branches of industries. They have been successfully used in numerous industrial applications, such as in aerospace, medicine, nuclear instrumentation and lately as pressure sensors in touch pads, mobile phones or as a tilt sensor in consumer electronics. Also in the automotive industry, piezoelectric elements are applied to monitor combustion in the development of internal combustion engines.

1.2. Intrinsic and extrinsic effect

The functional properties of piezoelectric materials depend on their microscopic nature [2]. In polycrystals (ceramics), each ceramic grain shows a domain configuration. In each domain, the orientation of dipoles is the same. These domains appear as a consequence of the ferroelectric nature of the ceramics. The different possible orientations of dipoles inside each domain depend on the crystallographic structure of the ceramics.

The dielectric and electromechanical properties of piezoelectric materials depend on the ability to change the macroscopic polarization under the application of an external electric or mechanical stimulus. The domain structure causes the appearance of two different processes of polarization change of the material: the so-called intrinsic and extrinsic contributions [3]. The intrinsic effect is due to the polarization change of each individual dipole, changing only its polarization magnitude, but without varying the limits of ferroelectric domains. It would be the one to happen if the whole grain were a single mono-domain, changing its polarization as a result of applying an electric field or an external strain. On the other hand, the extrinsic effect is easily defined as all responses that are different from the intrinsic response, which is mainly due to domain wall motion. Dipoles commute since they interchange their domain with a neighbouring domain.

The overall behaviour of a piezoelectric ceramic is the superposition of these two effects, the intrinsic and the extrinsic one. Most piezoelectric ceramics have excellent dielectric and electromechanical coefficients thanks to the contribution of the extrinsic effect. A good extrinsic contribution entails high value of piezoelectric coefficient, as is verified in ‘classical’ piezoceramics [4].

It is assumed that the intrinsic effect is a temperature independent behaviour, while the extrinsic effect, produced by the movement of domain walls, is temperature dependent [5]. Also, it is accepted that at very low temperatures the extrinsic contribution disappears because the domains wall freeze [6]. This is the reason why materials with potential high intrinsic contribution have been found since they are supposed to work at cryogenic temperatures. In this way, we would obtain good results in piezoelectric coefficients at low temperatures, because their fall is expected to be less steep.

To carry out this study two types of materials have been chosen. One group of commercial piezoceramics, which are used as reference materials for testing the experimental systems. The other group contains a set of lead-free, non-commercial materials on which this study is focused.

2. Materials evaluated

2.1. PZT

Lead zirconate titanate, with chemical formula $PbZr_xTi_{1-x}O_3$, commonly called PZT, is the most widely used piezoelectric material because it shows impressively good piezoelectric properties [7]. PZT has a perovskite crystal structure, each unit of which consists of a small tetravalent metal ion in a lattice of large divalent metal ions. In the case of PZT, the small tetravalent metal ion is titanium or zirconium. The large divalent metal ion is lead. Under compositional conditions that confer coexistence of tetragonal and rhombohedral crystallographic symmetries, called morphotropic phase boundary, the PZT exhibit enhanced properties.

PZT is an oxide based piezoelectric material developed by scientists at the Tokyo Institute of Technology around 1952. In comparison to the previously discovered oxide based piezoelectric material, the barium titanate ($BaTiO_3$ or BT), PZT exhibits greater sensitivity and higher operating temperature. Additionally, PZT system is compositionally engineered by doping resulting in a set of PZT-based materials with singular properties for specific application [2].

Due to their versatility, PZT-based materials govern the huge marked of piezoceramics. However, these materials have some drawbacks. The most important is their high lead content. The increasing success of PZT releases more and more lead, mainly in the form of either lead oxide or lead zirconate titanate into the environment. This occurs during calcination and sintering, where lead-oxide evaporates, during hard machining of components, and after usage with attendant problems of recycling and waste disposal. As a consequence, the European Union (EU) in 2003 included PZT in its legislature to be substituted as a hazardous substances by safe materials [8]. Hence, new applications of piezoelectric materials are called to use lead-free materials as alternative to lead-based ones.

Other, more important in the context of this work, drawback of commercial PZT-based piezoceramics is that the electromechanical properties of these materials dramatically fall when the temperature decrease to cryogenic region. That is the main reason why in this work we explore the properties of other piezoelectric materials.

2.2. BCTZ

As the most common piezoelectric system contains lead, and due to its toxicity, there is a demand for lead-free alternatives to PZT. However, the lead-free alternatives have to be reliable in long-term applications, and have to exhibit good piezoelectric performance. The BCTZ piezoelectric ceramics seem to be a

promising lead-free alternative piezoelectric material because it exhibit large piezoelectric response at room temperature [9].

In this work, piezoelectric ceramics based on $BaTiO_3$-$BaZrO_3$-$CaTiO_3$ (BCTZ) system are chosen because they show excellent properties at room temperature and, potentially, good intrinsic properties. This is, as already stated, the most important contribution at cryogenic temperatures. A set of different BCTZ samples, with compositions $Ba_{1-x}Ca_xTi_{0.9}Zr_{0.1}O_3$ (x = 0.1, 0.125, 0.15, 0.16, 0.17, 0.18) have been tested. This materials are synthesized in Instituto de Investigaciones en Materiales of the Universidad Nacional Autónoma de México, and some of their properties have been recently reported [10]. The better room temperature properties of this compositions are expected for x = 0.15 [11]. However, there are no studies to date about the performance of these materials at cryogenic temperatures. Thus, this study is novel itself in the materials science area. Moreover, it is important to point out that the BCTZ system has not been studied at all and not all compositions in the system have been synthesized and investigated.

The chosen compositions have an important difference compared with most common piezoelectric ceramics. The Curie temperature, which is the temperature at which the material changes from piezoelectric to non-piezoelectric, is less high as for most of the ceramics [12]. This leads to the assumption that if the Curie temperature is lower, then the piezoelectric properties at cryogenic temperatures might be better, since this phase change is accompanied by a peak of the dielectric constant. Due to this situation, a better performance is expected at cryogenic temperatures. With the Curie point being at a lower temperature, the corresponding peak of the dielectric constant will be also at a lower temperature. So, the analysed properties should achieve stronger values at cryogenic temperatures than compared to those with high Curie points.

3. Experimental procedure

3.1. Samples preparation

The poling process is the last phase of preparing a piezoelectric material. This process involves a lot of sub steps, to finally get a piezoelectric material of good properties.

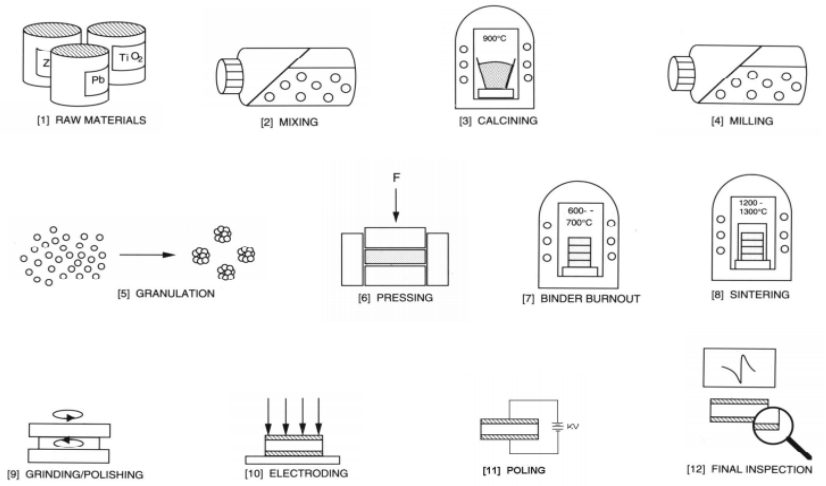

Figure 3.1.Piezoelectric manufacturing process [13]

In piezoelectric materials, dipoles with parallel orientation are grouped in a so called, Weiss domain. In regular ceramics, these domains are randomly grouped. This causes their response to an external electric field to tend to be zero, and this does not produce any change in the ceramic dimensions, which is the actual piezoelectric effect.

To obtain any piezoelectric response, dipoles have to be permanently aligned. In order to achieve this, it is resorted to a polarization process. The polarization process mainly depends on the values of the external electric field, the duration of the impact and the polarization temperature.

The external electric field will be different depending on the material. In our case we apply a voltage of 2000 V/mm [10]. As the electric air break occurs at ≈1500 V/mm, the polarization has to be performed in silicon oil. This step takes 30 minutes. The applied voltage and the polarization time are different for each material and so the manufacturer recommends for each case, specific voltages and polarization times.

The Curie temperature is the maximum exposure temperature for any piezoelectric ceramic. Above this temperature, all piezoelectric properties are lost. If the Curie temperature is high, the temperature at which the polarization is done is also high, but well below it. However, in the case of our non-commercial samples the polarization is done at room temperature, because the Curie temperature is not too high. On the other hand, in the case of commercial samples (PZT) the polarization was done at a higher temperature because the Curie temperature of the commercial materials is higher. The polarization of a piezoelectric ceramic consists of three main mechanisms: 1) The increase of

the intrinsic domain polarization, 2) the movement of domain walls and 3) the local changes of ferroelectric phase. In the figure 3.2 the difference in the domain configuration between polarized and non-polarized ceramic is shown.

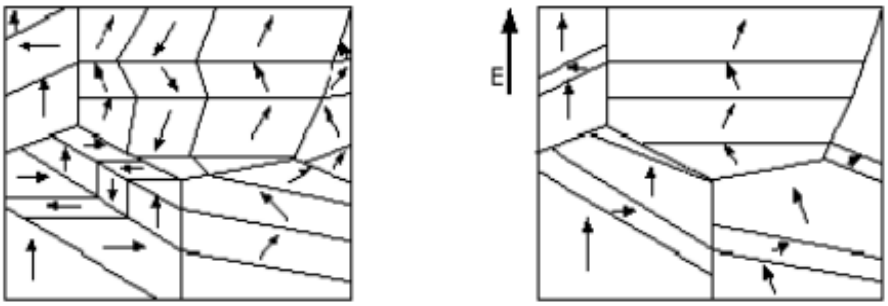

Figure 3.2.Non-polarized ceramic (left) and polarized ceramic (right) [14]

As it can be seen, the domains of a non-polarized ceramic are oriented in all directions. However, when the ceramic is polarized, its domains are reoriented to the direction of the electric field. When an Electric field is applied the ceramic domains are oriented exactly in its direction, but ones it no longer applies then the domains remain approximately in the same direction as it can be seen in figure 3.2.

3.2. Coefficients calculation

To obtain the piezoelectric coefficients, the knowledge of the fundamental equations is required, but these equations change depending on the geometry of the sample. So, if the sample is a rod, different equations will be used compared with e.g. a disk. For this reason, this section has been subdivided. But as our samples are disks only, the disk equations have been applied.

When a piezoelectric ceramic material is exposed to an AC electric field, its dimensions change cyclically. The frequency at which the piezoelectric ceramic vibrates most readily and most efficiently converts the electrical energy input into mechanical energy, is the resonance frequency.

The admittance is inversely proportional to the impedance, so when the impedance is minimum then the admittance is maximum. This is what happens at resonance conditions, since the impedance at that moment is always the minimum. On the other hand, at anti-resonance frequency the admittance is null

and the impedance is maximum. These admittance conditions will be used to obtain different piezoelectric coefficients.

In figure 3.3 the pattern of an element response can be seen. As the frequency is increased, the oscillations of the elements first approach the frequency at which impedance is minimum. This minimum impedance frequency, f_m is the frequency at which impedance in an electrical circuit describing the element is zero, if resistance caused by mechanical losses is ignored. The minimum impedance frequency also is the resonance frequency, f_r.
As the frequency increases, also the impedance increases to a maximum. This maximum impedance frequency is also the anti-resonance frequency, f_a.

The resonance frequency depends on the composition of the ceramic material and the volume and shape of the element. Generally, a thicker element has a lower resonance frequency than a thinner element of the same shape.

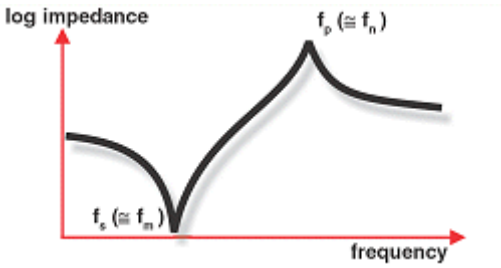

Figure 3.3 Impedance as a function of cycling frequency

3.2.1. Rod piezoelectric coefficients

In this part, it is exposed the piezoelectric coefficients used in this study to know how is the piezoelectric properties of the samples. These coefficients were obtained through the solution for the resonance and anti-resonance frequencies at the corresponding admittances [15].

Firstly, it has to be into account that when it is worked with a rods the geometry matters. So the figure 3.4 is an example of a rod sample.

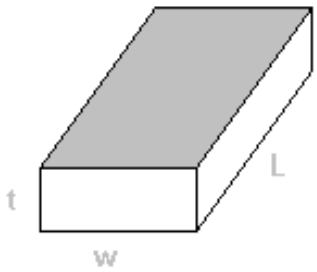

Figure 3.4. Rod of length L, width w, and thickness t [16]

The electrodes are placed on the largest surface, i.e. on the grey surface. It is arranged like this because the sample is studied in longitudinal mode.

To avoid the superposition of the different modes of longitudinal vibration in resonance, the rod must comply with the following geometrical conditions, w >L/3 and t >L/3 [15].

The used piezoelectric coefficients are the constant field compliance, coupling coefficient, the permittivity and the piezoelectric coefficient that are shown below respectively.

$$s_{11}^{E} = \left(\frac{n}{2l}\right)^{2} \frac{1}{\rho\left(f_r^{\,n}\right)^{2}} \tag{3.1}$$

Where l is the length, ρ is the density, f_r^n is the resonance frequency and 'n' represents the harmonic number, (n=1 fundamental, n=2 first harmonic, etc.).

$$k_{31} = \frac{1}{1-\sqrt{\frac{\tan\left(\gamma\alpha^{E}\right)}{\gamma\alpha^{E}}}} \tag{3.2}$$

The γ parameter depends on the angular frequency and length and α^E depends on the density and constant field compliance.

To determine the permittivity the capacity at frequency has to be measured where Y=0. This occurs at f = $2f_r$ and from C^P:

$$\varepsilon_{33}^{T} = \frac{t}{wl}\frac{1}{1-k_{31}^{2}}C^{P} \tag{3.3}$$

Rod of length l, width w, and thickness t

And finally the piezoelectric coefficient depends on the previous three coefficients in the next way:

$$d_{31}^{2} = \varepsilon_{33}^{T} s_{11}^{E} k_{31}^{2} \tag{3.4}$$

3.2.2. Disk piezoelectric coefficients

As it occurs with rods, a geometric condition is needed to avoid overlapping of the different vibration modes in a disk. All disks must comply with this geometric condition to ensure that d>5t, where d is the sample diameter and t is the thickness. The dimensions of the samples used in this work are referred to in table 3.1.

Ceramic	diameter(mm)	Thickness (mm)
BCTZ-0,1	10,26	1,230
BCTZ-0,125	10,27	1,230
BCTZ-0,15	10,25	1,310
BCTZ-0,16	10,27	1,260
BCTZ-0,17	10,31	1,280
BCTZ-0,18	10,18	1,330
BCTZ-1250º	10,03	1,580
BCTZ-1275º	10,02	1,590
BCTZ-1275º-2	10,04	1,440
BCTZ-1300º	9,94	1,590
PZ26	20,26	1,030

Table **3.1**. Geometric measurements of used samples.

The piezoelectric coefficients required in this study are Elastic compliance, the electromechanical coupling coefficient, the piezoelectric coefficient and the dielectric permittivity at constant stress that are shown below respectively.

$$\left(s_{11}^{E}\right)=\frac{1}{\rho\left(v^{P}\right)^{2}-\left[1-\left(v^{P}\right)^{2}\right]} \tag{3.5}$$

Where ρ is the density and the v_p is the planar velocity.

$$k_{31}^{2}=\frac{d_{31}^{2}}{\varepsilon_{33}^{T}*s_{11}^{E}} \tag{3.6}$$

$$d_{31} = e_{31}^{P} * (s_{11}^{E} + s_{12}^{E}) \tag{3.7}$$

$$\varepsilon_{33}^{T} = \varepsilon_{33}^{P} + \frac{2d_{31}^{2}}{(s_{11}^{E} + s_{12}^{E})} \tag{3.8}$$

The direction of the piezoelectric action or response depends upon the orientation of the poling axis. This orientation determines the direction of the action or response. To describe these directions, orthogonal axes are used, where 1 corresponds to the x-axis, 2 corresponds to the y-axis and 3 corresponds to the z-axis. However, in ceramic materials 1 and 2 are equivalent. The terms 4, 5 and 6 refer to various shear modes associated with the other three directions.

Some piezoelectric constitutive equations are the next [16]:

$$\{S\} = [s^{E}]\,\{T\} + [d^{T}]\{E\} \tag{3.9}$$

and

$$\{D\} = [d]\{T\} + [\epsilon^{T}]\,\{E\} \tag{3.10}$$

Where it can be seen the coefficients previous explained. The equation 3.9 is the elastic deformation and the equation 3.10 is the electric displacement. The one that really matter is the elastic deformation equation. The first part of both equations are constant, ergo, the applied tension is constant. So the important part of the equation 3.9 is which relates the piezoelectric coefficient with the electric field that results in the elastic deformation.

The electromechanical coupling coefficient k is the quantity of electric energy that becomes in a mechanical energy in ideal conditions, without taking into account the dielectric losses. The elastic compliance s is the deformation obtained only in implementing mechanic tension. The piezoelectric coefficient d is the relation between the applied tension and the deformation obtained as it can be seen in the equation 3.9.

3.3. Experimental system

The measurements of the resonance and anti-resonance frequencies, of the fundamental and the first harmonic, to evaluate the elasticity, the piezoelectric and dielectric coefficients as well as the dielectric losses, are performed in an experimental system that allows doing temperature sweeps from 390 K to 15 K.

This system consists of a water refrigerator and a Helium compressor with two vacuum pumps; one to create a relative vacuum and the other to create super vacuum. This setup is the cooling system that allows getting down to 15 K. Moreover, the system has a temperature controller to be able to do the temperature sweep in a controlled manner. The measurements of the low resonance frequency were performed with an impedance analyser. However, to calculate the dielectric properties a precision LCR was used.

The complete system is connected to a computer which is in charge of carrying out the measurements and saving the data for each temperature by an automatized process.

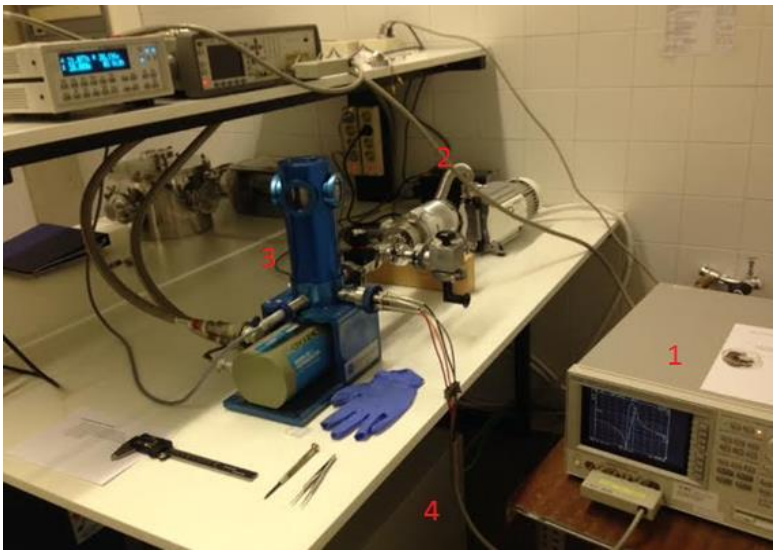

Figure 3.5. Experimental system (Impedance analyser, two vacuum pumps, cold finger and compressor).

Figure 3.7 shows the different components of the laboratory which have been mentioned before in this section. To get a clear idea the components are numbered:

1. Impedance analyser
2. Two vacuum pumps
3. Cold finger
4. Compressor, also under the table is the water pomp.

The samples are placed into the so-called cold finger, but the actual cold finger is what is inside the blue housing, inside the other metallic housing. There are two housings to ensure the maximum possible isolation.

The contacts in the resonance measurements are small pins that touch the sample in the middle and are isolated from the cold finger, decreasing thus the noise introduction in the measurement. For that reason, the temperature changes, produced by radiation, occur slowly. To guarantee a good thermal stability of the sample, the system remains stabilizing for 10 minutes, after the control of temperature has been reached. This time depends on the temperature steps that we are using, for a step of 5 K, the system spends 10 minutes stabilizing.

For each temperature, the resonance and anti-resonance frequencies of the fundamental and the first harmonic are measured, as well as the parameters of the equivalent circuit of the fundamental mode. The capacitance is measured at low frequencies and intermediate frequencies, at which the mechanic admittance is zero, but also at high frequencies. The values of the real and imaginary part of the admittance at 1 KHz are measured, which are ε' and ε" respectively.

To better understand how the experimental process works, it will be explained in chronological order.

1. Before placing the sample in the laboratory setup, the side wall of each sample has to be sanded. By doing this, the frontal and back face are not in electric contact.
2. Once the samples have been polarized and sanded, they have to be placed inside the cold finger.
3. The resonance and anti-resonance frequencies of the fundamental and harmonic waves are looked up in the impedance analyser to introduce the values into the computer together with the sample parameters (area, radius and thickness). If the dielectric coefficients are measured then this step is not needed, since the resonance frequency is not necessary and the impedance analyser is not used.
4. The air taps have to be turned off.
5. The first vacuum pump is turned on. In this way, a vacuum is created in the system. After a few minutes, the other vacuum pump is turned on to create a super vacuum inside the system where the sample is located.

6. Once the super vacuum is created, the water pump is connected and one minute later also the compressor is connected.
7. Now the experiment is ready to start.

4. Results

In this section contains all the graphs obtained in the laboratory including the dielectric and resonance coefficients. Once all the dielectric coefficients were calculated, all the samples were polarized to be able to obtain the piezoelectric coefficients. It must be taken into account that every graph has a duration of at least two days, ergo, the graphics obtainment process took weeks. It has to be clarified that there are two groups of non-commercial samples, here called Solid State and Pechini. Both of them are BCTZ but they were obtained from different processing route, resulting in materials with the same composition but different microstructure; for instance, different grain size.

4.1. Dielectric response

Before starting with the piezoelectric measurements, the dielectric measurements have been carried out, to give us a primary idea of what the behaviour of the samples will be. If the dielectric coefficient is good versus the temperature, also will be the piezoelectric coefficients.

To display the results of the dielectric coefficients and to obtain the most information graphs have been plotted which show the behaviour of the dielectric coefficient and the losses vs the temperature. These measurements have been done at different frequencies, to know the best working frequency of each sample.

When we talk about dielectric coefficients and losses, we address also admittance, since the admittance, as said in the section 3.2, is inversely proportional to impedance. Impedance can be divided into two parts, the real one and the imaginary part

$$Y = G + iB \tag{4.1}$$

where G is the real part and B the imaginary part. The real part is the resistance that corresponds to the dielectric losses and the imaginary part which is the capacity which in turn is the dielectric constant. So, if the dielectric losses are

high then a lot of energy is dissipated in form of heat. This means that when an electric current circulates into a piezoelectric sample, this sample vibrate less and also heat the environment. The dielectric losses at very low temperatures are quite to zero since at these temperatures only there is the intrinsic part.

4.1.1. Solid state

To show all the information of the six samples a graph of each sample showing its behaviour has been plotted. It shows the dielectric constant but also the dielectric losses at different frequencies, more concretely, at 100 Hz, 1, 10 and 100 KHz and 1 MHz. Additionally, two graphs have been created to compare the six samples among them, showing their behaviour at 1 KHz.

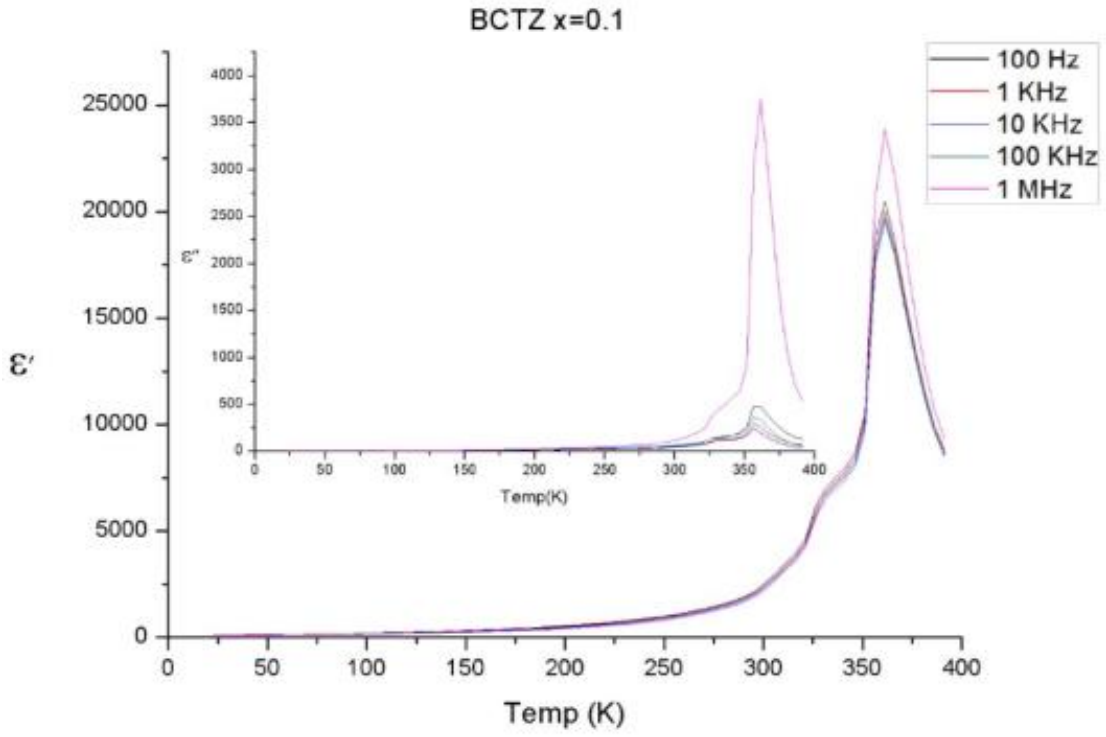

Figure 4.1.Dielectric coefficient and losses vs temperature of BCTZ x=0.1

4. Results

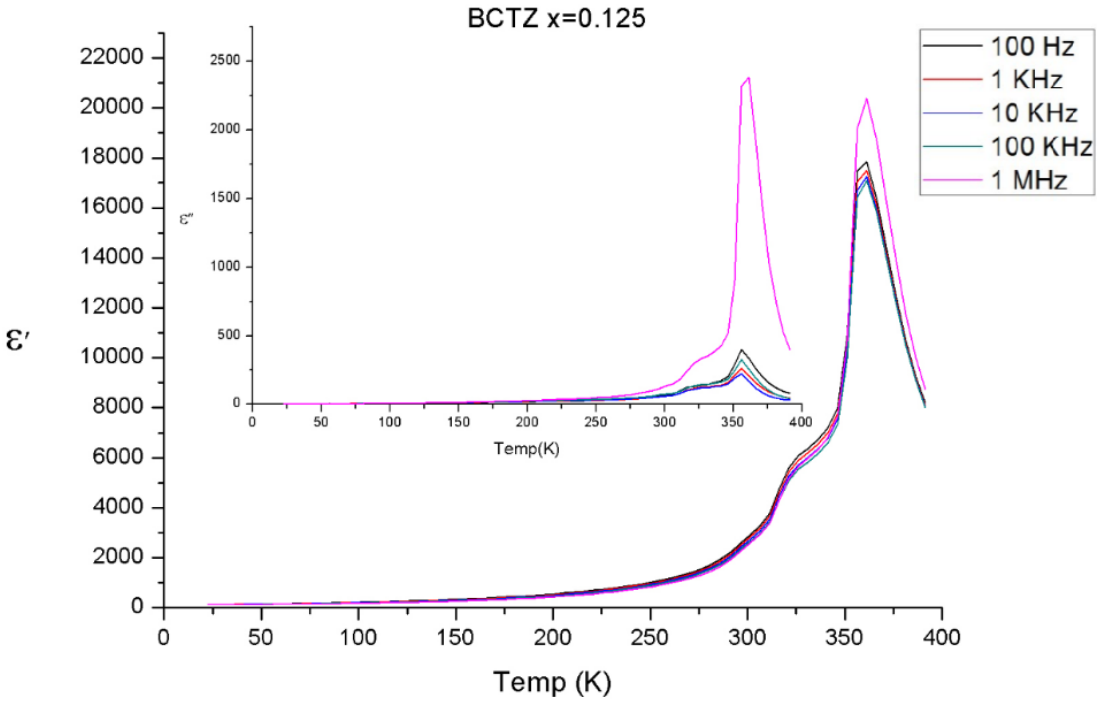

Figure 4.2.Dielectric coefficient and losses vs temperature of BCTZ x=0.125

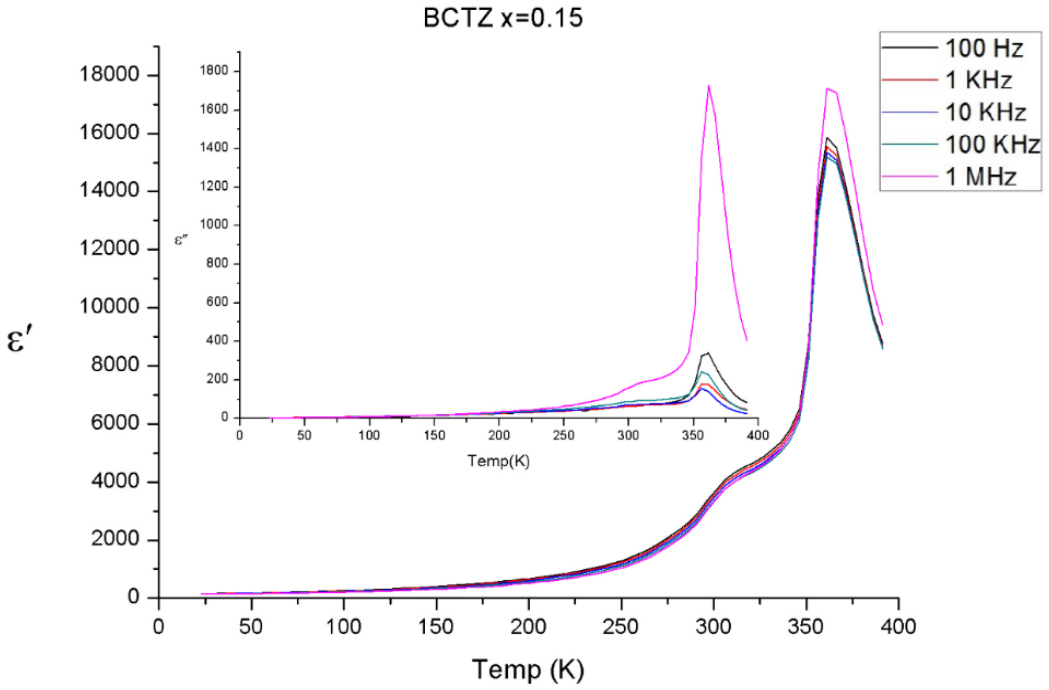

Figure 4.3.Dielectric coefficient and losses vs temperature of BCTZ x=0.1

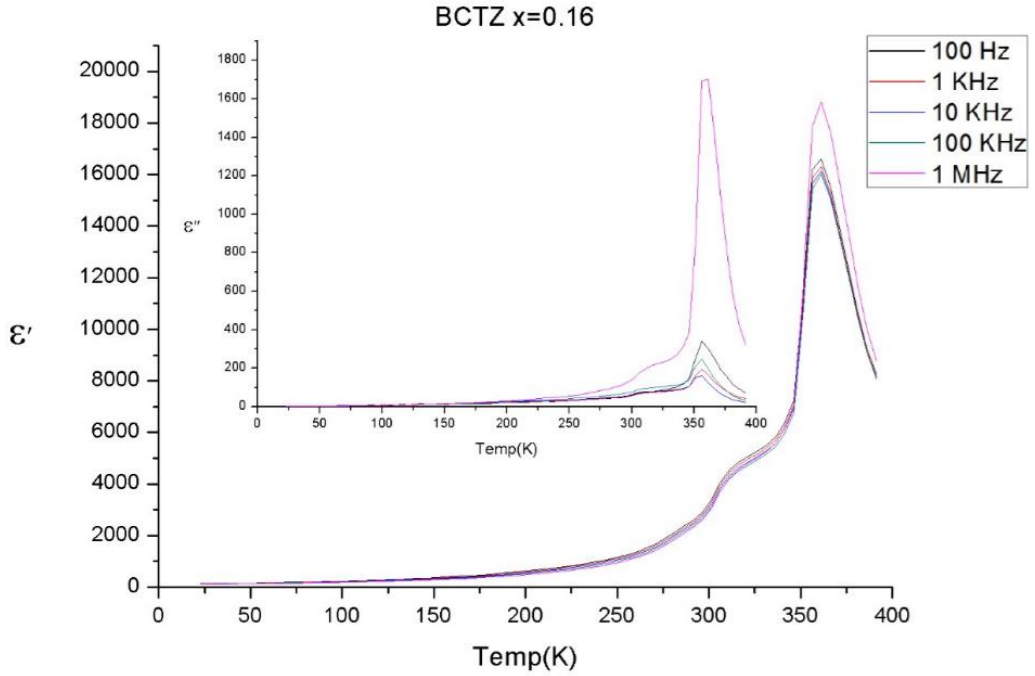

Figure 4.4.Dielectric coefficient and losses vs temperature of BCTZ x=0.16

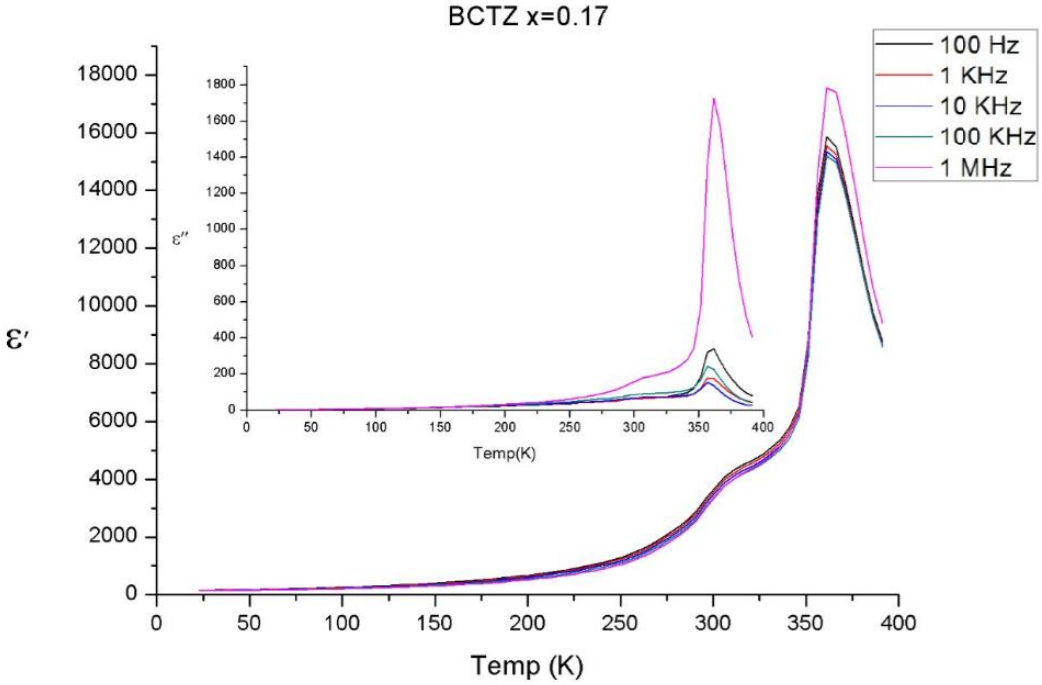

Figure 4.5 Dielectric coefficient and losses vs temperature of BCTZ x=0.17

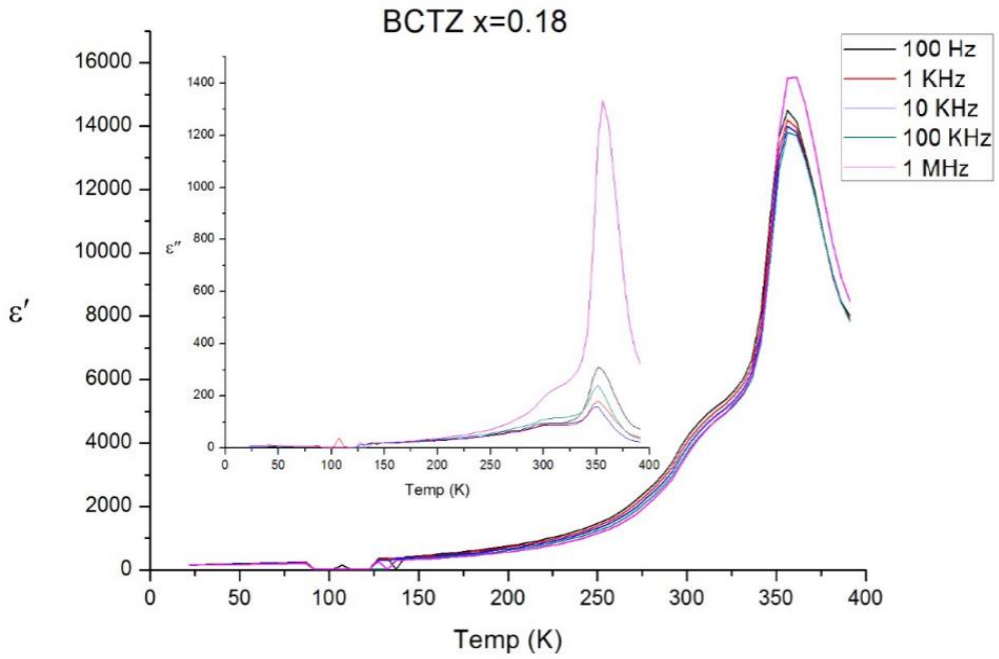

Figure 4.6 Dielectric coefficient and losses vs temperature of BCTZ x=0.18

As it can be seen in the previous graphs, all samples have a very similar behaviour vs temperature. Also, all samples peak at same temperature; 360 K, since all samples have a low Curie temperature. Despite this, the abrupt descent of properties couldn't be avoided. This causes the properties to be worse than expected at cryogenic temperatures.

To compare all samples among them, the graphs 4.7 and 4.8 have been plotted. One to display the dielectric coefficient and the other to display the dielectric losses. Both of them show the same behaviour at a 1 KHz frequency. To get a better idea of the samples, also an enlargement of the most important parts of the graph has been zoomed out at cryogenic temperature and at room temperature. In this way, the coefficient at cryogenic temperature can be clearly appreciated, which is the main reason of this study.

These results are not positive and lead to the conclusion that the piezoelectric properties of these samples will only be very small.

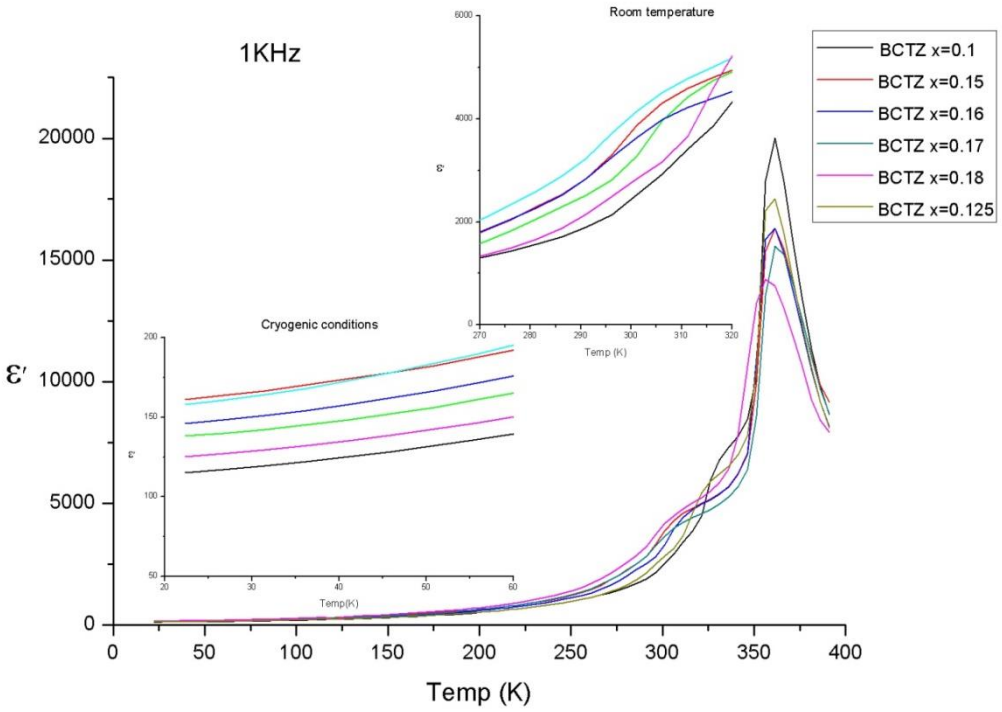

Figure 4.7 Dielectric coefficient of BCTZ vs temperature at 1 KHz

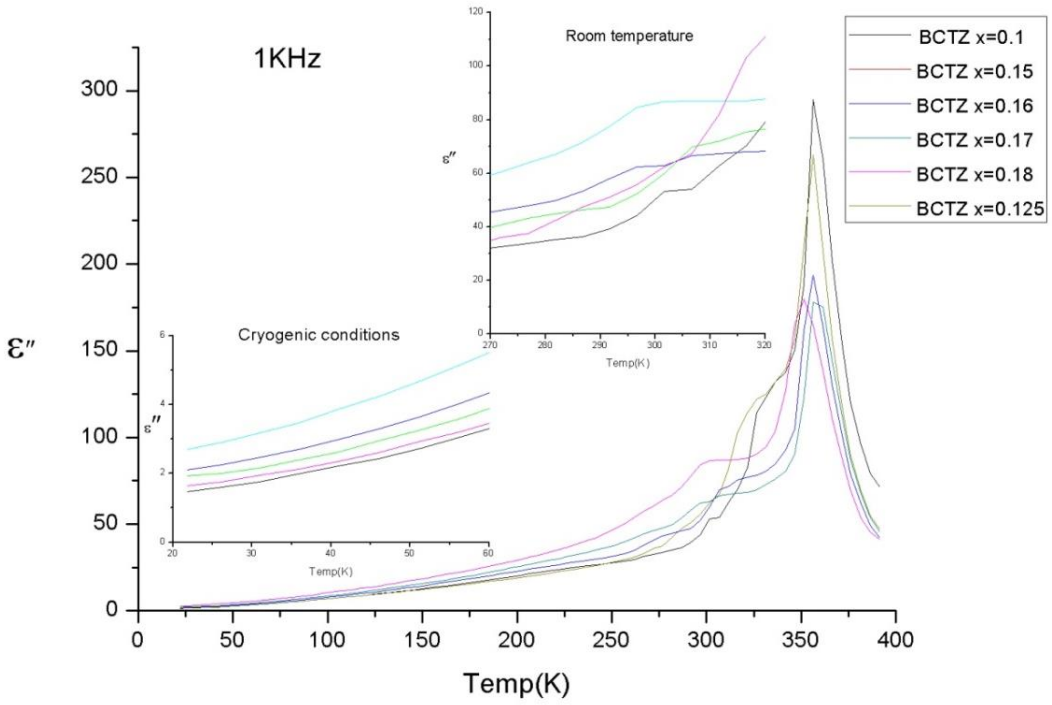

Figure 4.8.Dielectric losses of BCTZ vs temperature at 1KHz

4.1.2. Pechini

To get the dielectric coefficient and dielectric losses of these different types of samples, the same process as the one preformed with the solid state samples is repeated.

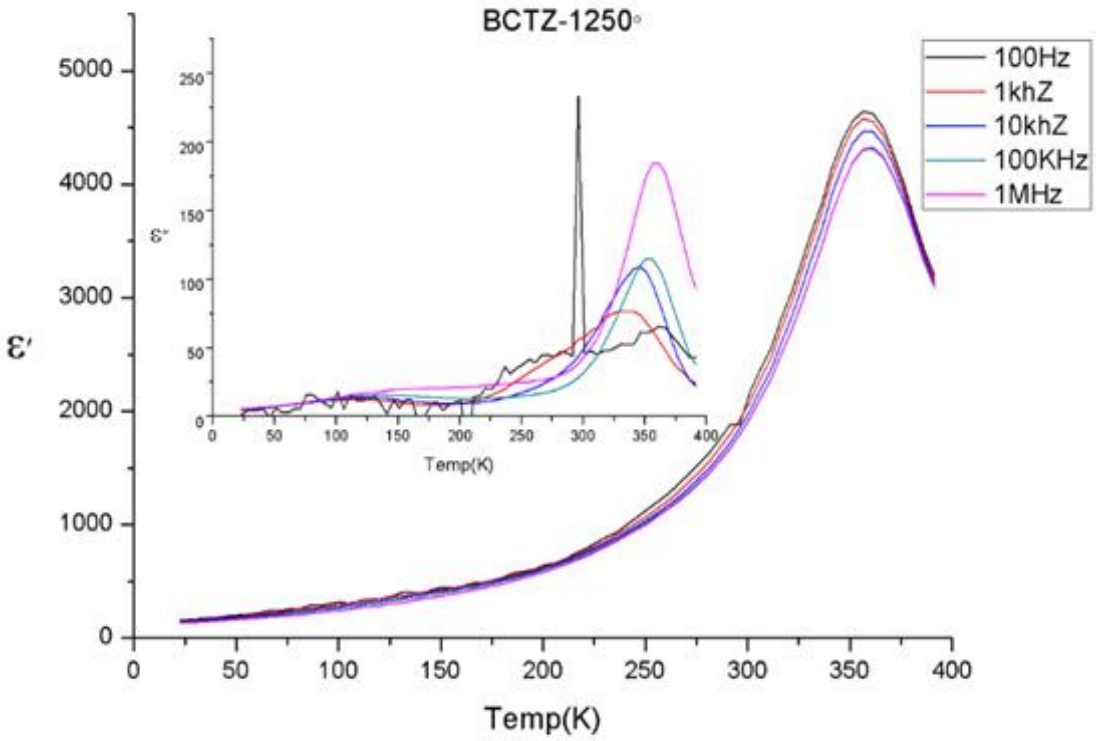

Figure 4.9.Dielectric coefficient and losses of BCTZ-1250º

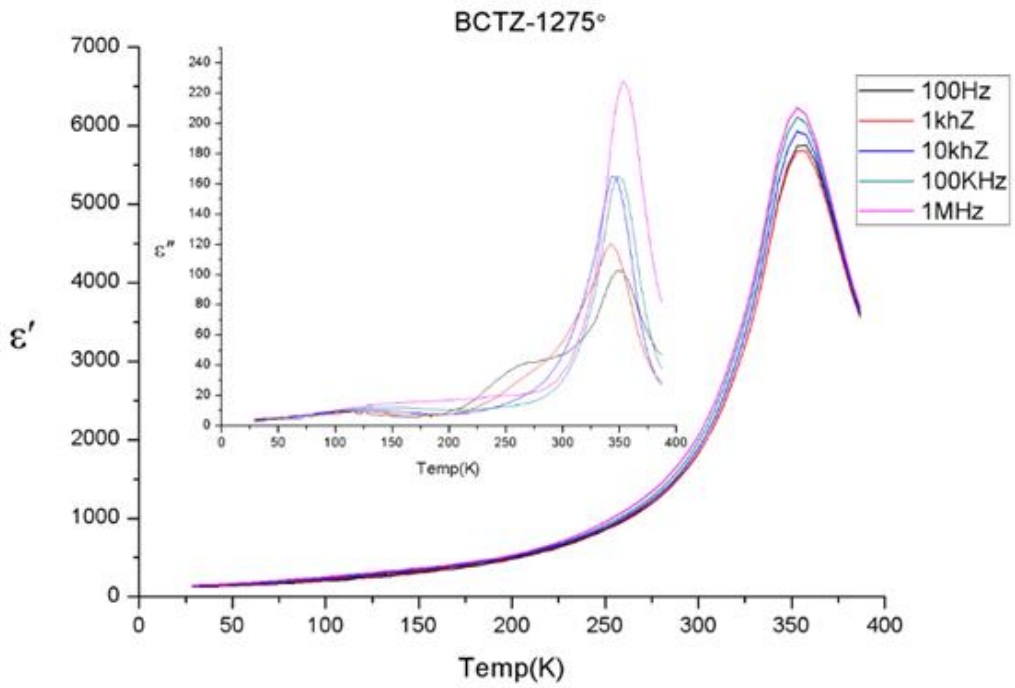

Figure 4.10 Dielectric coefficient and losses of BCTZ-1275º

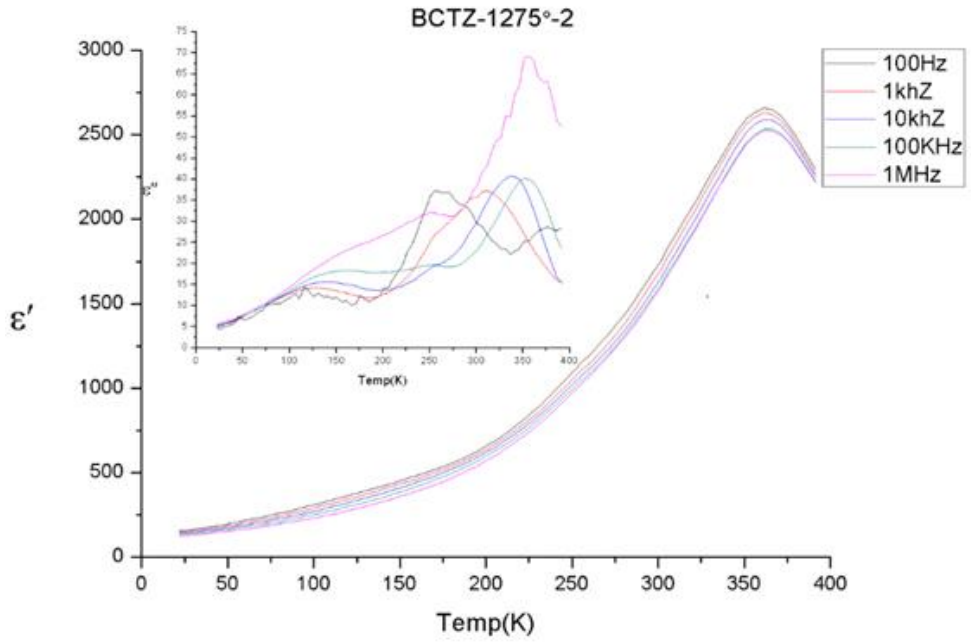

Figure 4.11. Dielectric coefficient and losses of BCTZ-1275º-2

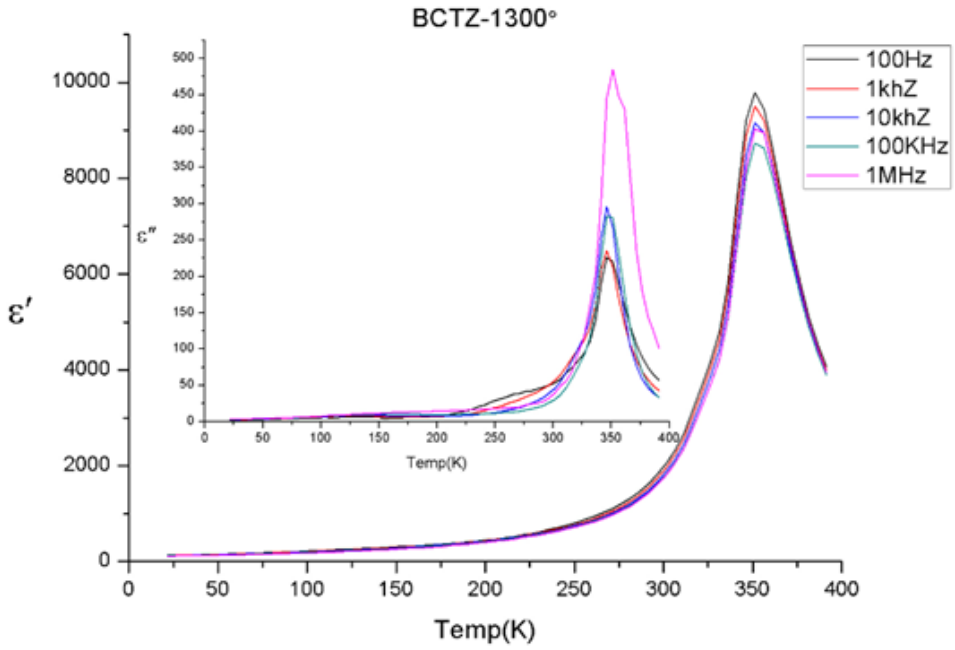

Figure 4.12. Dielectric coefficient and losses of BCTZ-1300º

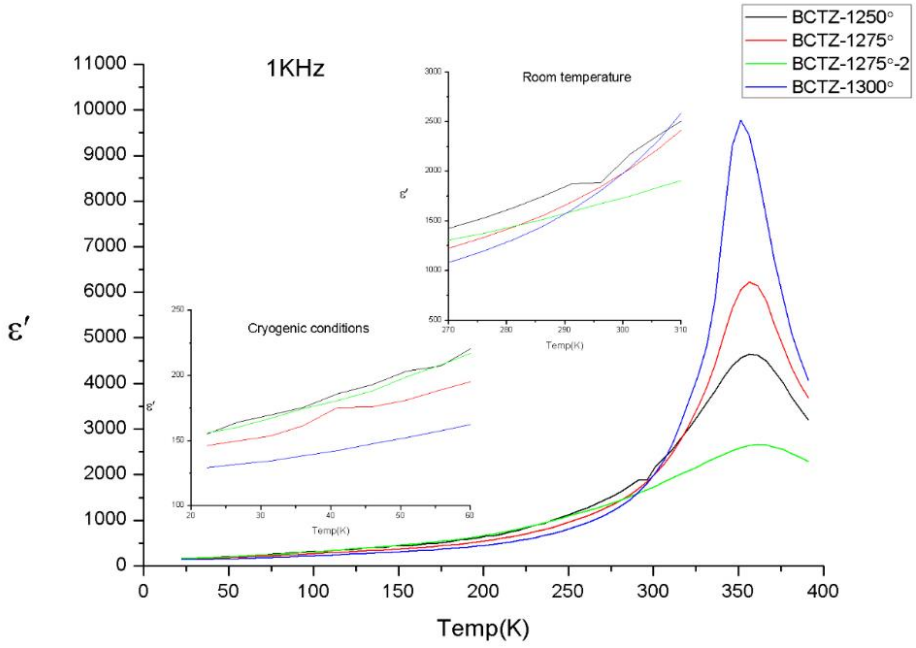

Figure 4.13.Dielectric coefficient of BCTZ vs temperature at 1 KHz

The graphs 4.9 to 4.12 display the behaviour of each sample at different frequencies versus the temperature. As it can be seen in these graphs, the properties of these samples are not good. In fact, the properties of all samples at room temperature are much worse than then ones of the Solid-State samples. The peak of properties, which occurs just before the Curie temperature, is found at 360 K. Else, this peak doesn't show very good properties as happens with the other samples, but this causes the fall of the properties to be much less steep.

In the graph 4.13 all Pechini samples are compared in order to find which one works best. To give a better readability, the main parts of the graphs have been zoomed out for cryogenic temperatures and room temperatures. From here we can evaluate which sample has the best properties. The sample BCTZ-1300º has the biggest dielectric constant but as the temperature falls, this sample is the one with the steepest fall towards cryogenic temperatures.

None of these Pechini samples could work at cryogenic temperatures since the properties at cryogenic temperatures are not strong enough and for that reason it is not worth doing the piezoelectric study of these samples.

4.2. Electromechanical response

In spite of all dielectric coefficients have not been as good as expected, it has decided to determine the piezoelectric coefficients of one type of samples, the Solid State since that ones were designed to have good piezoelectric properties at cryogenic temperature.

Once the dielectric coefficient and losses have been calculated to get a first idea of these samples, it is time to obtain the piezoelectric coefficient. To be able to calculate this coefficient, some previous preparation steps must be done.

In order to record all properties of the samples a Matlab program is necessary. The Matlab program has the purpose of processing all the data obtained in the lab. Those data, which come out of the experiment are many and of a great variety. They contain data that is used to calculate the coefficients explained before, as the resonance and anti-resonance frequency, the capacity and the planar velocity v^p at each temperature and much more information. To obtain the coefficients it is used the admittance exact solutions, choosing the suitable forms of the constitutive equations according to contour conditions and the samples geometry [15].

The admittance equation is the next:

$$Y = \frac{-i\omega\varepsilon_{33}^{P}\pi a^2}{t}\frac{2\left(k^{P}\right)^2}{1-\sigma^{P}-J_1^{C}} - \frac{-i\omega\varepsilon_{33}^{P}\pi a^2}{t} \tag{4.2}$$

Admittance also can be written as $Y = Y_{Mec} + Y_{Elect}$, where:

$$Y_{Mec} = \frac{-i\omega\varepsilon_{33}^{P}\pi a^2}{t}\frac{2\left(k^{P}\right)^2}{1-\sigma^{P}-J_1^{C}} \tag{4.3}$$

and

$$Y_{Elect} = \frac{i\omega\varepsilon_{33}^{P}\pi a^2}{t} \tag{4.4}$$

Where a and t are the radius and thickness of the ceramic material, respectively; ε_{33}^{P} is the planar permittivity, k^{p} is the radial planar coupling coefficient, ω is the angular frequency, σ^{p} is the planar Poisson coefficient and J_1^{c} is the cylindrical Bessel function of order 1 [15].

Using the equation of admittance and applying the resonance and anti-resonance conditions. In the resonance frequency the impedance at that moment is always the minimum, ergo the admittance is maximum ($Y\rightarrow\infty$). On the other hand, at anti-resonance frequency the admittance is null (Y=0) and the impedance is maximum. Applying these two conditions to the admittance equation and with the resonance and anti-resonance frequency which are obtained directly from the laboratory as said before, it is obtained the transcendental equations.

($Y\rightarrow\infty$)
$$J_1^{C}(z) = 1-\sigma^{P} \tag{4.5}$$

and

(Y=0) $$J_1^C(z) = 1 - \sigma^P - 2 * \left(k^P\right)^2 \quad (4.6)$$

Solving the equation 4.4 the planar Poisson coefficient σ^P is obtained. As σ^P and v^p have been estimated, K^p can be determined. Also Thanks to definitions of Planar Poisson coefficient and the planar velocity [15], s_{11}^E can be determined. And finally to determine the planar dielectric coefficient ε_{33}^P it is measured the ceramic capacity at which the Y_{mec} is zero. So, the next condition must be met:

$$1-\sigma^P - J_1^c(z) = \infty \quad (4.7)$$

From the formulas explained before and with the help of the Matlab program all the piezoelectric coefficients, as S_{11E}, d_{31}, $k_{31,}$ ε_{33}^P could be obtained.

Unlike in the case of the dielectric coefficients, for the measurement of the resonance frequencies a resistance analyser has to be available in order to calculate the resonance and anti-resonance frequencies of each sample.

To obtain the maximum amount of information of all samples we have tried to plot a graph for each coefficient explained before. Nevertheless, at some point in time during the experiment, the sample lost the contact with the sample holder, so some data became corrupt and some coefficients e.g. k_{31} were been affected. For this reason, it was decided to choose only three coefficients. ε_{33P}, d_{31}, S_{11E} were selected because of their importance and because they reflect the behaviour of all samples in a good way. On the other hand, if the results had been good, the process of the samples would have been repeated, in order to obtain all the coefficients without any disruption. But due to the lack of time and because the coefficients obtained were not satisfactory, this needn't to be done.

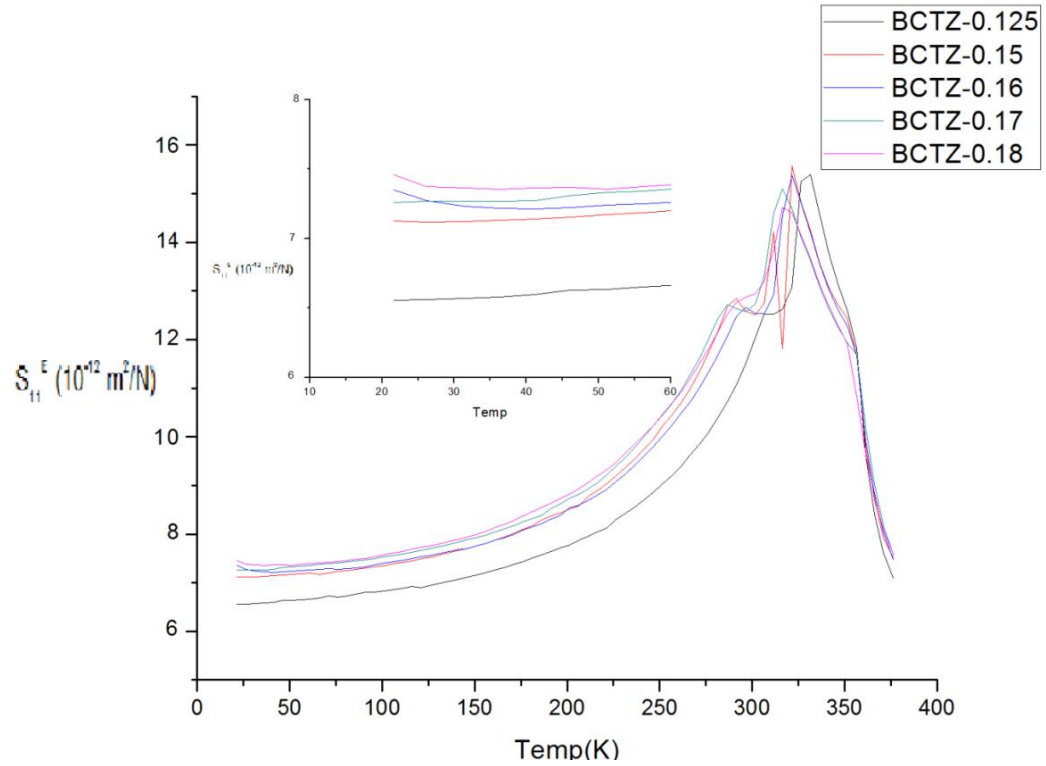

Figure 4.14. Elastic compliance S_{11}^E vs temperature at 1 KHz

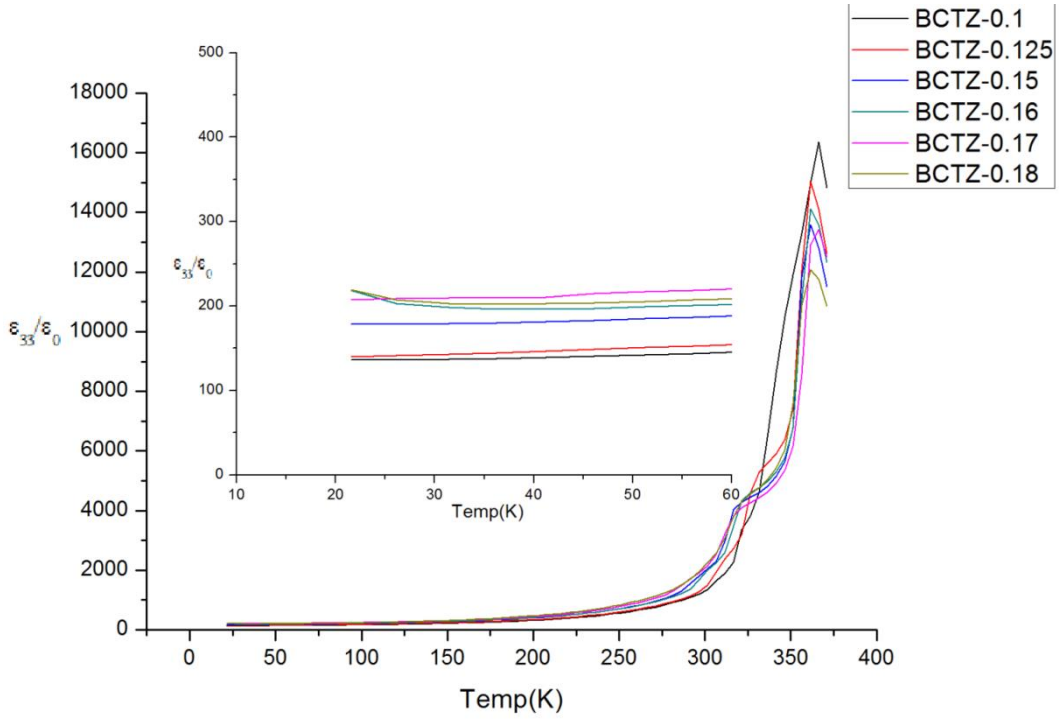

Figure 4.15.$\varepsilon_{33}/\varepsilon_0$ vs temperature at 1 KHz

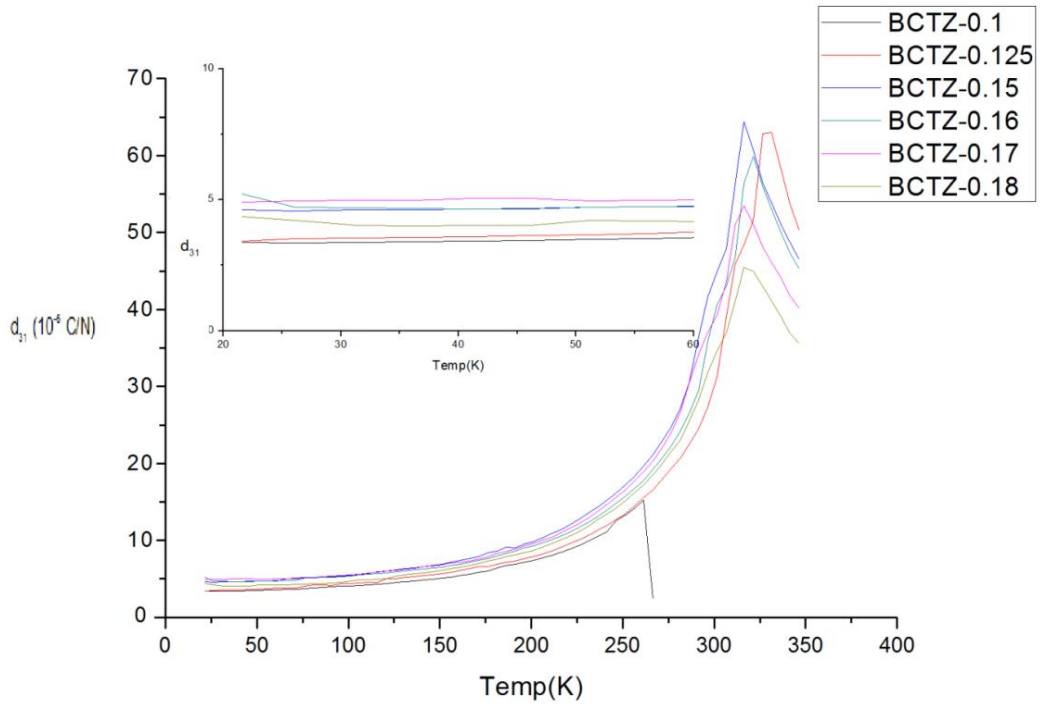

Figure 4.16.Piezoelectric coefficient vs temperature at 1 KHz

From the graphs 4.14, 4.15 and 4.16 it can be clearly understood how the behaviour of all samples is. To get a better idea an enlargement has been done, but this time only at cryogenic temperatures.

The graphs 4.15 and 4.16 show the relative permittivity and the piezoelectric coefficient respectively. As it can be seen, these coefficients are almost constant at very low temperatures, so although the desired temperature were i.e. 150 K, the coefficients would still be bad. The elastic compliance at cryogenic temperatures also is too small. These results are too small and are very far from the expected which are needed for its correct working under cryogenic conditions.

5. Conclusions

This study has done in the Piezoelectric Materials laboratory of Physics Department of the UPC and it has used different samples of BCTZ to check its piezoelectric properties for an aeronautical application.

These samples were chemically designed to have a good behaviour at low temperatures by increasing the intrinsic effect, since this contribution does not depend on temperature. In addition, the samples were created to have a low Curie temperature and thus to improve the properties at cryogenic temperatures in order to use the samples under cryogenic conditions. Despite this design selection, the samples did not show the expected properties. The values of the measured properties of the samples have decreased in an incredible way, as it can be seen in the previous graphs of the piezoelectric coefficients.

So, in spite of these samples were created especially for this study, the results have not been appropriate for the intended application. The studied samples have displayed almost the same behaviour as any other commercial samples.

These results in all the piezoelectric coefficients, which were not expected in Solid State samples, have demonstrated that it is very difficult to find a piezoelectric ceramic material that has good enough properties at room temperature as to have enough properties at cryogenic temperatures. However, the main objective of the study can’t be discarded, which is to find a piezoelectric material that works efficiently at cryogenic temperatures, because notwithstanding there are many other materials besides ceramics that could work at cryogenic conditions, like piezoelectric crystals which have good properties. The problem with crystals is that they’re very expensive in comparison with ceramic materials. Latter was one of the main reasons why ceramics were chosen instead of crystal for this study.

In conclusion, the chosen piezoelectric ceramics don’t have shown good enough piezoelectric properties to work in the best possible way under cryogenic conditions. We would have had to find a ceramic material with an extremely big intrinsic effect, so the decline towards low temperatures might have been less steep. Ceramics are not appropriate for this purpose and crystalline materials are too expensive for a real-world application. Though it seems to be rather difficult, the next step should be to find a different material that might work correctly at cryogenic conditions.

6. Bibliography

[1] D. Ortega, Historia del ultrasonido: El caso chileno', *Revista chilena de Radiología*, Vol.10 nº 2, 2004

[2] B. Jaffe, W. R. Cock Jr and H. Jaffe, *Piezoelectric ceramics*, London, 1971.

[3] J. E. García, *Extrinsic contribution and instability properties in lead-based and lead-free piezoceramics*, Materials 8, 7821, Barcelona, 2015.

[4] D. A. Ochoa, J. E. Garcia, R. Pérez, and A. Albareda, *Influence of extrinsic contribution on the macroscopic properties of hard and soft lead zirconate titanate ceramics*, IEEE Transactions on Ultrasonics, Ferroelectrics and Frequency Control 55, 2732, Barcelona, 2008.

[5] Q. M. Zhang, H. Wang, N. Kim, and L. E. Cross, *Direct evaluation of domain wall and intrinsic contributions to the dielectric and piezoelectric response and their temperature dependence on lead zirconate titanate*, Journal of Applied Physics 75, 454, 1994.

[6] X. L. Zhang, Z. X. Chen, L. E. Cross, and W. A. Schulze, *Dielectric and piezoelectric properties of modified lead zirconate titanate ceramics from 4.2 to 300 K*. Journal of Materials Science 18, 968, 1983.

[7] J. Rodel, W. Jo, K. T. P. Seifert, E.-M. Anton, T. Granzow, and D. Damjanovic, *Perspective on the development of lead-free piezoceramics*, Journal of the American Ceramics Society 92, 1153–1177, 2009.

[8] EU-Directive 2002/95/EC: *Restriction of the Use of Certain Hazardous Substances in Electrical and Electronic Equipment (RoHS)*, Off. J. Eur. Union, 46 [L37] 19–23, 2003.

[9] J. Rodel, K. G. Webber, R. Dittmer, W. Jo, M. Kimura, and D. Damjanovic, *Transferring lead-free piezoelectric ceramics into application*, Journal of the European Ceramics Society 35, 1659, 2015.

[10] A. Reyes-Montero, L. Pardo, R. López-Juárez, A. M. González, S. O. Rea-López, M. P. Cruz, and M. E. Villafuerte-Castrejón, *Sub-10 μm grain size, $Ba_{1-x}Ca_xTi_{0.9}Zr_{0.1}O_3$ (x = 0.10 and x = 0.15) piezoceramics processed using a reduced thermal treatment*. Smart Materirials and Structures 24, 065033, 2015.

[11] W. Liu, and X. Ren, *Large piezoelectric effect in Pb-Free ceramics*. Physical Review Letter 103, 257602,2009.

[12] M. E. Villafuerte-Castrejón, E. Morán, A. Reyes-Montero, R. Vivar-Ocampo, J.-A. Peña-Jiménez, S.-O. Rea-López, and L. Pardo, *Towards lead-free piezoceramics: facing a synthesis challenge*, Materials 9, 21, 2016.

6. Bibliography

[13] Piezoceramic division, *High quality components and materials for the electronic industry*, Ferroperm, scientific magazine, Kvistard, 1995.

[14] Juliewatty Mohamed, *Processing and Testing electroceramics*, Malasya, 2016

[15] American National Standards Institute, *IEEE Standard on Piezoelectricity*, Institute of Electrical and Electronics Engineers, New York 1987.

[16] D. A. Ochoa*, Respuesta extrínseca y comportamiento no lineal en materiales cerámicos piezoeléctricos*, Tesis Doctoral, Universitat Politècnica de Catalunya, 2009.